Optical design of the 75 MeV Eindhoven Racetrack Microtron

G.A. Webers, J.L. Delhez, J.I.M. Botman, H.L. Hagedoorn
Eindhoven University of Technology
P.O. Box 513, 5600 MB Eindhoven
The Netherlands

Abstract

A 75 MeV racetrack microtron is being designed and constructed at the Eindhoven University of Technology. This microtron will serve as injector for the storage ring EUTERPE. The microtron contains two inhomogeneous bending magnets which are rotated in the median plane. In this paper we will present the optical design of the machine using a first order matrix theory to describe the focusing forces, including fringe field effects. Optimization of the machine acceptance in the horizontal and vertical plane yields the optimum shape of the magnet poles, which are currently under construction. The results from matrix theory are verified by numerical orbit tracking using the measured field map. Also an analysis of the effect of alignment errors will be given.

I. INTRODUCTION

At the Eindhoven University of Technology, a 75 MeV racetrack microtron (RTME) is being designed and constructed (see Figure 1). This microtron will serve as injector for the electron storage ring EUTERPE [1]. A similar RTM (25 MeV) is simultaneously being built for a FEL project [2]. The electrons are injected from a 10 MeV medical linac into the microtron and are accelerated in a 2998 MHz standing wave cavity with an accelerating voltage of 5 MeV. Two phase-locked 2.2 MW magnetrons will be used to power the 10 MeV injector linac and the cavity separately. This will be sufficient to accelerate 10 mA current. From numerical simulations it is seen that the accepted momentum spread $\Delta p/p$ is about 1% at injection (10 MeV), which is reduced to 0.15% at extraction (75 MeV).

The magnetic field consists of 2-sector magnets, separated by a drift space of 0.99 m. The dimensions of the magnets are 50x150x45 cm^3. The gap and magnetic field in sector I and II are respectively, 20 mm, 0.51 T and 17 mm, 0.60 T. This field increase is realized by pole shaping. Due to the magnet design there is a field dip, i.e. the magnetic field in the center is lower than the field near the edges. The magnets are rotated at an angle τ in the median plane to obtain proper 360^0 bending [3]. The dashed curve in the orbit pattern in Figure 1 shows were the high field region II will end, such that the exit angle at extraction is 2τ. The number of orbits is 13 and the orbit separation is 60.6 mm, which is sufficient for beam monitoring and steering.

At the front of the magnets, clamps are mounted to shield the magnetic field in the drift space.

The vacuum system will be made of aluminium and consists of a central vacuum chamber, two wedged shaped chambers and the vacuum boxes in the magnets. A 400 l/s turbo pump will be connected to the central vacuum chamber to obtain a pressure in the 10^{-6} mbar regime.

In the center of the microtron a correction magnet (CM) will be placed to correct the bending angle of each orbit separately. For beam diagnostics we will use Beam Position (BP) monitors.

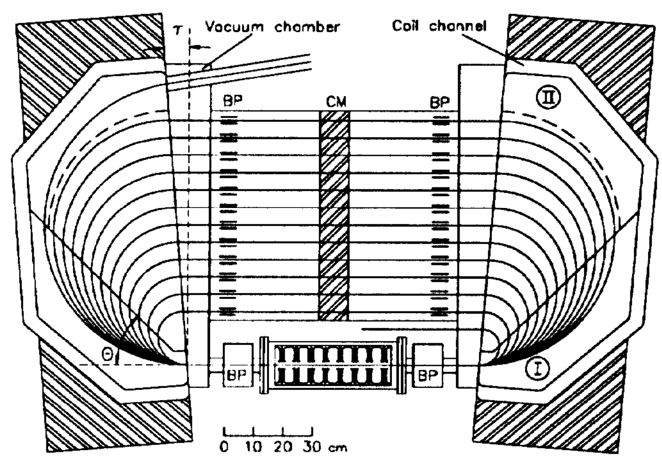

Figure 1: *Median plane view of the Eindhoven Racetrack Microtron*

Table 1: Main RTME parameters

RF frequency	2998 MHz
Drift length	0.99 m
Injection energy	10 MeV
Extraction energy	75 MeV
Accelerating voltage	5 MV
Number of orbits	13
Magnetic field (sector I/II)	0.51 T / 0.60 T
Mode number	2
Orbit separation	60.6 mm

The 2-sector configuration is described by the ratio $a = B_{II}/B_I$ and the angle θ between the boundary, separating sector I and II, and the cavity axis. The tilt angle τ is related to a and θ by the condition of 360^0 bending. The injection energy, accelerating voltage and magnetic field are related by the isochronism condition, i.e. the

0-7803-1203-1/93$03.00 © 1993 IEEE

path length of each orbit is an integer multiple of the RF wave length λ. The path length difference between two successive orbits is $h\lambda$ with h the mode number. In the case of the RTME we have chosen h=2 in order to limit the number of orbits and to have a sufficient orbit separation.

II. TRANSVERSE MOTION

The shape of the magnetic field is determined by the parameters a and θ. To estimate the optimum $\hat{a}$ and $\hat{\theta}$, we optimized the machine acceptance using a first order matrix theory including the defocusing effect of the fringe fields [3]. Using a drift length of 0.99 m, we found $\hat{a}$=1.17 and $\hat{\theta}=45^0$ ($\tau=4.5^0$) which yields a horizontal acceptance of about 100 mm.mrad and a vertical acceptance of about 50 mm.mrad. The vertical acceptance is mainly limited by the mismatch in phase space between the injection orbit (10 MeV) and the first orbit (15 MeV), but this can easily be compensated by placing a quadrupole in the center of the microtron. The defocusing effect in the horizontal plane is small, but even this can be compensated by using a quadrupole doublet.

From the numerical calculations it is seen that the horizontal acceptance is (almost) not affected by a momentum spread $\Delta p/p$ in the range of -1%..1%.

As a check, we performed numerical orbit calculations and estimated the horizontal and vertical tunes ν_x and ν_z. As input we used a field map, generated from field profiles in 2D cross sections of the magnet. We used the analytical tool of conformal mapping [4] to estimate these profiles. In Figure 2 we plotted ν_x and ν_z versus energy for each orbit separately. In the range 20..70 MeV we see a good agreement between the theoretical results and the results obtained from numerical orbit tracking using the computer code HIATT [5]. The discrepancy in ν_x at lower energies is probably caused by the fringe fields which force a deviation of the reference orbit.

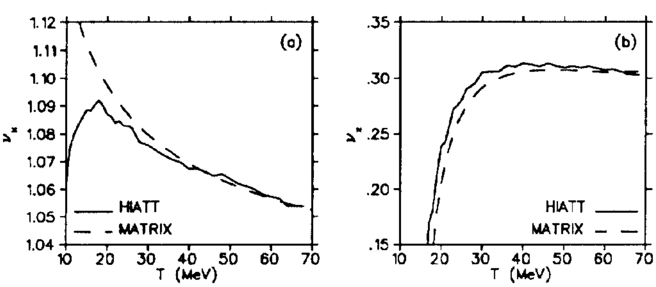

Figure 2: *(a) ν_x and (b) ν_z versus kinetic energy T from numerical orbit tracking (solid) and 1[st] order matrix theory (dashed)*

To estimate the effect of the realistic 3D magnetic field distribution we used the computer code RELAX3D [6] which solves the potential distribution, i.e. the magnetic field distribution for non-saturated cases. The results of this code for 2D cross sections are in good agreement with Conformal Mapping, but the accuracy of the 3D results is limited by the number of mesh points, and will not be used therefore.

III. LONGITUDINAL MOTION

An important feature of a microtron is the longitudinal focusing effect which is obtained by proper timing of the injection process with respect to the RF wave in the cavity. To study the longitudinal motion, we solved numerically the difference equations. In Figure 3a we plotted the phase ϕ and energy spread ΔT at injection, which correspond to an extraction energy which is close (within 1%) to 75 MeV. In Figure 3b we plotted the corresponding phase space at extraction. Here we used a synchronous phase $\phi_s=9^0$ which gives a maximum separatrix area (area occupied in phase space at injection) of about 30 deg% at 10 MeV. The dashed curve is the separatrix as derived by a Hamiltonian derivation of the equations of motion.

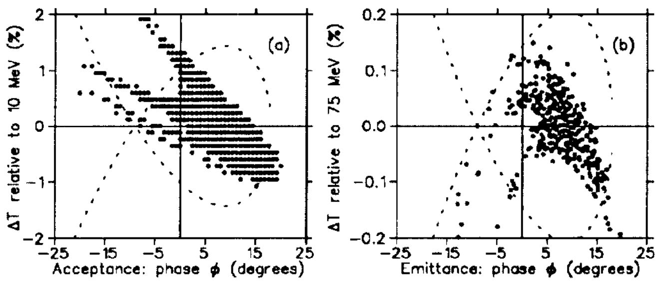

Figure 3: *Longitudinal phase space at (a) injection (10 MeV) and (b) at extraction (75 MeV) with $\phi_s=9^0$*

So far we neglected the effect that the relativistic velocity β <1. Including this effect, the stable region in phase space at injection shifts towards smaller ΔT-values by 0.4%, but the separatrix area does not change.

Factors that may disturb the longitudinal motion are (i) path length deviations due to the field dip (3%) in the center of the magnet and (ii) (time-dependant) cavity voltage variations. The effect of the field dip is (partly) compensated by a (small) increase of the magnetic field. The remaining path length error is less than 6 mm and shows some oscillatory behaviour versus energy. From numerical simulations we see that the separatrix area is almost not affected by this remaining path length deviation. This implies that no isochronism corrections are required so we only need a central correction magnet for proper orbit bending.

Similar calculations have been performed for a cavity voltage variation $\Delta V/V$. For a constant voltage variation we find $\Delta V/V \leq 2\%$ is allowed in the case of the RTME. Including a harmonic voltage variation with frequency Δf and amplitude $\Delta V/V$, we find a maximum $\Delta V/V \approx 0.7\%$ at Δf=1 MHz and a maximum $\Delta V/V$=0.3% at Δf=20 MHz. Note that the latter affects each micro pulse since the revolution time is about 0.14 μs (7 MHz). Expected voltage variations, due to cavity tuning errors and generator power variations, are in the order of 1%.

IV. MEASUREMENTS

At this moment, the 2-sector magnets are available for magnetic field measurements. The measuring equipment consists of a Hall probe, mounted on a computer controlled X-Y table. In order to check the transverse optics, we measured the field map of one magnet in a mesh of 70x110 cm with mesh sizes of 10 mm in both directions. From numerical orbit tracking we see that the exit angles are about 30 mrad due to the field dip. This effect is (partly) compensated by adjusting τ to 3.6^0. In this case, we find $\nu_z \approx 0.31$ and $\nu_x \approx 1.1$ in the range 20..70 MeV, which is in agreement with the design values. To obtain the matrix for a full acceleration process of 13 orbits, we estimated the transfer matrix for each orbit separately and added the matrix describing the cavity. The corresponding horizontal and vertical acceptance are plotted in Figure 4. Here the injection energy is varied while the extraction energy is fixed at 70 MeV, the last full orbit. The solid curves refer to the design values while the dashed ones are derived from the measured field map and we see a very good agreement.

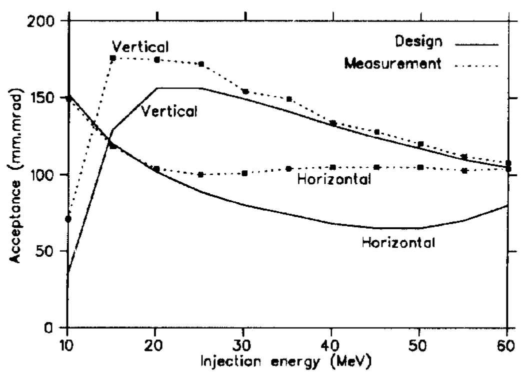

Figure 4: *Horizontal and vertical acceptance versus injection energy. The extraction energy is fixed at 70 MeV*

To check the numerical orbit tracking results, we used the Hall probe as reference particle and measured directly the orbit and its gradient. The tunes ν_x and ν_z estimated from these measurements are in agreement with the results given above.

V. MISALIGNMENTS

To study the effect of misalignments we used the description of Lobb [7] and extended this model to mechanical errors specific for our 2-sector geometry (δa, $\delta\theta$). Limiting ourselves to the horizontal motion, it is seen that δa (in the order of 1%) has by far the largest effect. In order to compensate an asymmetric δa (i.e. left and right magnet) we need for each magnet a separate correction possibility. A symmetric δa is easily compensated by chosing a different τ. This is still possible since the vacuum chamber is not constructed yet.

Compared to the alignment errors, the field dip of about 3% gives by far the largest contribution to the path length, total bending angle and exit position. Due to the small gap it is not profitable to use correction coils inside the magnets and therefore we investigate the use of one central correction magnet. Since the effect on the longitudinal motion is small, we only need a correction magnet to bend at most 40 mrad at 45 MeV in the horizontal plane. Since we want to have the possibility to control each orbit separately, we designed an array of 12 (iron cored) magnets. A (part of the) cross section is shown in Figure 5 where the dots represent the designed beam center. Using a bending length of 12 cm and a gap of 2 cm, the maximum field is about 500 Gauss to correct for the field dip. From POISSON [8] calculations we have seen that the homogeneity in the center of each pole is about 0.5% within 10 mm. The magnetic field drops to about 1% in the neighbouring cell.

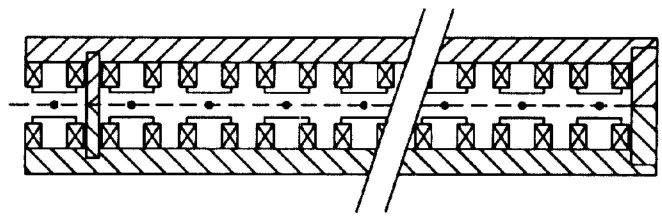

Figure 5: *Designed central correction magnet*

To estimate the optimum correction strengths we used the Least Squares Minimization method. It is found that, after one full turn, the path length difference with respect to the unperturbed case, is less than 2 mm, the orbit shift is less than 1 mm and the angle with respect to the cavity axis is less than 1 mrad, in the range 10..75 MeV.

VI. CONCLUSIONS

In this paper, we described the layout of a 75 MeV racetrack microtron. The optical design is discussed and the effect of alignment/construction errors is mentioned. Magnetic field measurements have been done to check the theoretical design and a good agreement is found.

VII. REFERENCES

[1] B. Xi et.al. - Nucl. Instr. and Meth. B68 (1992) 101-104

[2] J.I.M. Botman et.al. - Nucl. Instr. and Meth. A318 (1992) 358-363

[3] J.L. Delhez et. al. - Nucl. Instr. and Meth. B68 (1992) 96-100

[4] G.A. Webers et. al. - Nucl. Instr. and Meth. B68 (1992) 83-86

[5] G.A. Webers - '*HIATT users manual*, TUE (1992)

[6] C.J. Kost and F.W. Jones - '*RELAX user guide and reference manual*', Computing document of Triumf, Vancouver, Canada (1988)

[7] D.E. Lobb - Nucl. Instr. and Meth. 87 (1970) 59-72

[8] M.T. Menzel and H.K. Stokes, '*User's guide for the POISSON/SUPERFISH Group of Codes*', LA-UR-87-115 (1987)